Macromolecules
ARTICLE

Macromolecules **2010**, *43*, 9063–9070 **9063**
DOI: 10.1021/ma1015984

Water Content and Buildup of Poly(diallyldimethylammonium chloride)/Poly(sodium 4-styrenesulfonate) and Poly(allylamine hydrochloride)/Poly(sodium 4-styrenesulfonate) Polyelectrolyte Multilayers Studied by an in Situ Combination of a Quartz Crystal Microbalance with Dissipation Monitoring and Spectroscopic Ellipsometry

Jagoba J. Iturri Ramos,[†] Stefan Stahl,[†,§] Ralf P. Richter,[†,‡] and Sergio E. Moya*[,†]

[†]*Biosurfaces Unit, CIC biomaGUNE, Paseo Miramón 182, 20009 San Sebastian, Gipuzkoa, Spain, and* [‡]*Max-Planck-Institute for Metals Research, Stuttgart, Heisenbergstrasse 3, 70569 Stuttgart, Germany.* [§]*Present address: Ludwig-Maximilians Universität, Amalienstrasse 54, 80799 Munich, Germany.*

Received July 15, 2010; Revised Manuscript Received September 7, 2010

ABSTRACT: The buildup of polyelectrolyte multilayers (PEMs), fabricated by the layer-by-layer (LBL) assembly, was followed in situ by the combination of a quartz crystal microbalance with dissipation monitoring (QCM-D) and spectroscopic ellipsometry in a single device. PEMs composed of poly(allylamine hydrochloride) (PAH) and poly(sodium 4-styrenesulfonate) (PSS) polyelectrolyte pairs and of poly(diallyldimethyl ammonium chloride) (PDADMAC) and PSS were built up to 17 layers. The combination of ellipsometry and QCM-D allowed simultaneous determination of the acoustic mass, which comprises both the mass of the polymer and solvent, and the optical mass which corresponds to the polymer mass alone. From these parameters, the hydration of the PEM was calculated layer by layer. The linearly growing PAH/PSS PEMs showed a constant absolute content of water throughout the assembly, while the relative contribution of water to the PEM mass content approached zero, when grown in 0.5 M NaCl. Rinses with water between polyelectrolyte deposition steps resulted in a hydration of approximately 40%. The supralinearly growing PDADMAC/PSS PEMs exhibited a remarkable dependence of the hydration on the polyelectrolyte that was deposited last. Implications for the mechanism of assembly of the PEMs are discussed.

Introduction

Since their introduction in the 90s, polyelectrolyte multilayers (PEMs) based on the alternate assembly of oppositely charged polyelectrolytes by means of the so-called layer-by-layer (LBL) technique have gained the attention of the scientific community as an inexpensive, simple and robust route for surface modification and as a tool for device fabrication.[1−12]

Despite ample research on these systems, there are basic questions related to their assembly that still remain unknown. It has been shown that for certain combinations of polyelectrolytes the growth of the multilayers scales linearly with the number of assembled layers.[13,14] This is the case, for example, for multilayers composed of poly(allylamine hydrochloride) (PAH) and poly(sodium 4-styrenesulfonate) (PSS). For other polyelectrolyte pairs, such as poly(diallyldimethylammonium chloride) (PDADMAC) combined with PSS, the growth of the multilayer has been found to follow an exponential trend when assembly takes place in the presence of certain concentrations of NaCl in an aqueous medium. Such exponential behavior has been demonstrated to occur as a result of the diffusion of at least one of the polyelectrolytes in and out of the previously assembled layers:[15−20] since the whole film is acting as an active volume and is capable absorbing the depositing polymer, the mass that binds per deposition cycle increases as a function of the total film mass.

The quartz crystal microbalance with dissipation monitoring (QCM-D) has proven to be a powerful technique to follow the growth of PEMs and to characterize the mechanism of their assembly.[21−23] The QCM-D responses, i.e., the resonance frequency f and the energy dissipation D of the shear oscillatory motion of a piezoelectric quartz crystal sensor, change upon adsorption or desorption of material on the surface of that sensor. The measured parameters are highly sensitive to the mass and the mechanical properties of the surface-bound layer. Mass resolution for example is on the order of a few ng/cm^2. Owing to its acousto-mechanical transducer principle, the QCM-D technique is sensitive not only to the adsorbed molecules but also to the solvent that is retained within or hydrodynamically coupled to the surface-bound film. It is hence often difficult to extract the adsorbed molecular mass from the QCM frequency response alone, i.e., to separate the contribution of the adsorbate from the contribution of the solvent that is coupled to it.

Polyelectrolytes are charged molecules with hydrated monomers. Furthermore, water can be trapped in cavities within a polyelectrolyte multilayer, either between polyelectrolyte molecules forming a given layer or between subsequent layers during assembly.[24,25] Besides, it is not known how much the deposition of a layer on a PEM will affect the content of water of the previously assembled layers. Hence, to reach a more comprehensive knowledge of the mechanism of polyelectrolyte assembly, additional and complementary experimental techniques are required.

Spectroscopic ellipsometry is also a frequently used technique for characterizing the assembly of thin films at interfaces.[26,27] Ellipsometry is an optical technique, where the change in the polarization state of an incident light wave upon reflection

*Corresponding author. E-mail: smoya@cicbiomagune.es.

Published on Web 10/07/2010

at an interface is measured. The polarization change is measured in terms of the ellipsometric angles ψ and Δ as a function of the wavelength λ, which can be detected with high accuracy. The simultaneous in situ determination of ψ and Δ can provide, by proper data treatment, quantitative information on the refractive index, thickness and mass of thin films at planar interfaces.[28,29] As ellipsometry is sensitive to differences in the optical density between adsorbate and bulk solution, it essentially senses the adsorbate mass. Therefore, by comparison of the values for the masses obtained by both QCM-D and ellipsometry, the water content of a PEM can be calculated.

The work by Halthur and Elofsson[30] illustrates how the growth of a multilayer composed of biocompatible polymers could be followed layer by layer by applying both techniques in separate experiments. The growth of m_{opt} and m_{QCM} of PEMs was studied on different samples because both methods could not be easily applied simultaneously for technical reasons.

Here, we present the combination of spectroscopic ellipsometry and QCM-D in a single device to study how the content in water, or aqueous solvent, and the amount of deposited polyelectrolyte vary along the layer-by-layer formation of a PEM. First, the growth of multilayers composed of the PAH/PSS polyelectrolyte pair was studied and their aqueous solvent content quantified. Here we found that the change in the ionic strength during washing had a distinct influence on the incorporation of water in the PEM. Our characterization approach was then extended to multilayers composed of PDADMAC as polycation and PSS as polyanion. For these systems, we observe an unexpectedly complex dependence of the aqueous solvent content on multilayer growth.

PAH/PSS and PDADMAC/PSS are among the most studied polyelectrolyte systems in PEMs. PAH is a weak polyelectrolyte with primary amines as pending groups while PDADMAC is a strong polyelectrolyte whose charge originates from quaternary amines. Their respective multilayered films display very different properties[31,32] with regard to stability, pH response, elasticity, and conductivity. The combination of ellipsometry and QCM-D in a single device brings the advantage that the responses of both techniques are measured in parallel and in real time from the same sample under identical experimental conditions. This allows, in particular, for the time-resolved quantification of variations in the aqueous solvent content during the buildup of PEMs. Based on these results, basic aspects regarding multilayer buildup will be addressed for both PDADMAC/PSS and PAH/PSS multilayers.

Materials and Methods

Materials. Poly(diallyldimethylammoniumchloride) [PDADMAC 20% in water, $M_w \sim (2-3.5) \times 10^5$ kDa], poly(sodium 4-styrenesulfonate) [PSS, $M_w \sim 70$ kDa], and poly(allylamine hydrochloride) [PAH, $M_w \sim 15$ kDa] were purchased from Aldrich. Sodium chloride was purchased from Fluka. All reagents were used without further purification.

In Situ Combination of QCM-D and Ellipsometry. The formation of polyelectrolyte multilayers was monitored simultaneously, by QCM-D and ellipsometry, on the same surface and in liquid environment. Measurements were performed using a purpose designed flow cell (Q-Sense AB, Västra Frölunda, Sweden) with a total volume of ~300 μL. The flow cell was attached to a Q-Sense E1 setup, providing access to QCM-D data and mounted on a spectroscopic rotating compensator ellipsometer (M2000 V, Woollam, NE, U.S.A.), providing access to ellipsometric data. QCM-D data, Δf and ΔD, were acquired at six overtones, $i = 3, 5, ..., 13$, corresponding to resonance frequencies of $f_i \approx 15, 25, ..., 65$ MHz) simultaneously, with subsecond time resolution. Ellipsometric data, Δ and ψ, were acquired over a wavelength range from $\lambda = 380$ to 1000 nm, simultaneously, at 65° as angle of incidence, and with a time resolution of ~5 s. The working temperature was 23 °C.

Layer-by-Layer Assembly. PEMs were assembled on QCM-D sensors (QSX335, Q-Sense AB) with a fundamental resonance frequency of about 4.95 MHz. The sensor coating was purpose designed for ellipsometric measurements and consisted of an opaque bottom layer of titanium, a thin (~1 nm) titania interlayer, and a top layer of about 80 nm silica. The sensors were pretreated with UV/ozone (BioForce Nanosciences, Ames, IA, U.S.A.) for 30 min.

The LBL assembly was performed by alternately passing 1 mg/mL in 0.5 M NaCl polyelectrolyte solutions and washing in Milli-Q water or 0.5 M NaCl solutions with a peristaltic pump (ISM935C, Ismatec, Zürich, Switzerland) through the flow cell. Two different assembly protocols were followed. In the first protocol, a 0.5 M NaCl solution was used for washing steps between the deposition of each individual polyelectrolyte and the sample was washed with pure water only at the end of the assembly. In the second protocol, the sample was rinsed with pure water after the deposition of each layer.

Quantitative Evaluation of QCM-D Data. The Sauerbrey equation[33] links frequency shifts and adsorbed masses per unit area in a very simple way:

$$m_{QCM} = -C \frac{\Delta f_i}{i} \quad (1)$$

with the mass sensitivity constant, $C = 18.06 \pm 0.15$ ng·cm^{-2}·Hz^{-1} for sensors with a resonance frequency of 4.95 ± 0.02 MHz, and the overtone number i. The normalized frequency shifts, $\Delta f = \Delta f_i/i$, for the third overtone were employed to determine m_{QCM}. This acoustic mass comprises the mass of the adsorbed polymer and the mass of the solvent that is trapped inside or hydrodynamically coupled to the polymer film. The applicability of eq 1 is limited to rigid films. For soft and dissipative films, more complex models would be required that account for the viscoelastic properties of the film.[34,35] For the PEMs investigated here, we found the ratio of dissipation and normalized frequency shifts, $\Delta D/-\Delta f$, to be smaller than 0.2×10^{-6}/Hz, indicating that eq 1 is a good approximation. The application of the viscoelastic models to selected data sets (details of the modeling procedure are given in ref 36) corroborated that the Sauerbrey equation is indeed a good approximation for our films, with an error below 5%. The experimental noise was typically below 2 ng/cm^2.

The film thickness was further determined by

$$d_{QCM} = m_{QCM}/\rho_{PEM} \quad (2)$$

with $\rho_{PEM} = 1.0$ g/cm^3 being the density of the solvated polymer film. In their pure form, the employed polymers exhibit densities between 1.0 and 1.2 g/cm^3, while the density of water or salt solutions is 1.0 g/cm^3. Equation 2 hence overestimates the thickness by at most 20%.

Quantitative Evaluation of Ellipsometric Data. Bound masses were determined by numerical fitting of the ellipsometric data to a multilayer model. Data were fitted over the accessible wavelength spectrum, using the software CompleteEASE (Woollam). The model relates the measured ellipsometric responses, Δ and ψ as a function of λ, to the optical properties of the sensor surface, the adsorbed film, and the surrounding solution. The glass windows in the fluid cell were verified not to perturb the polarization of the probing light beam, and the optical properties of the sensor coating were calibrated prior to each measurement, as described elsewhere.[37]

To extract the properties of the adsorbed polymer film from the ellipsometric response, a five-layer model was used. The layers represented the bulk solution, the polymer film, and the three coating layers (silica, titania, and titanium) on the sensor that interact with the light beam. The PEM was treated as a single layer, which we assumed to be transparent and homogeneous (Cauchy medium), with a given thickness, d_{opt}, a

wavelength-dependent refractive index, $n_{PEM}(\lambda) = A_{PEM} + B_{PEM}/(\lambda/\mu m)^2$, and a negligible extinction coefficient ($k_{PEM} = 0$). d_{opt}, A_{PEM}, and B_{PEM} were fitted simultaneously. The semi-infinite bulk solution was also treated as a transparent Cauchy medium, with a refractive index of $n_{sol}(\lambda) = A_{sol} + B_{sol}/(\lambda/\mu m)^2$. For water, $A_{sol} = 1.323$ and $B_{sol} = 0.00322$ were estimated from the literature.[38] For 0.5 M NaCl solutions, $A_{sol} = 1.328$ and $B_{sol} = 0.00322$ were employed.[39] The optical properties and thicknesses of the sensor's coating layers were fixed to the values established during calibration.

The adsorbed mass per unit area was determined from de Fejter's equation:[40]

$$m_{opt} = \frac{d_{opt}(n_{PEM} - n_{sol})}{dn/dc} \quad (3)$$

To calculate m_{opt}, we employed the refractive indices at $\lambda = 632.5$ nm and used a refractive index increment of $dn/dc = 0.150$ cm^3/g.[30] We note that the errors associated with d_{opt} and $n_{PEM} - n_{solvent}$ can be rather high for films that exhibit only a few nanometers in thickness. We observed also that the absolute values

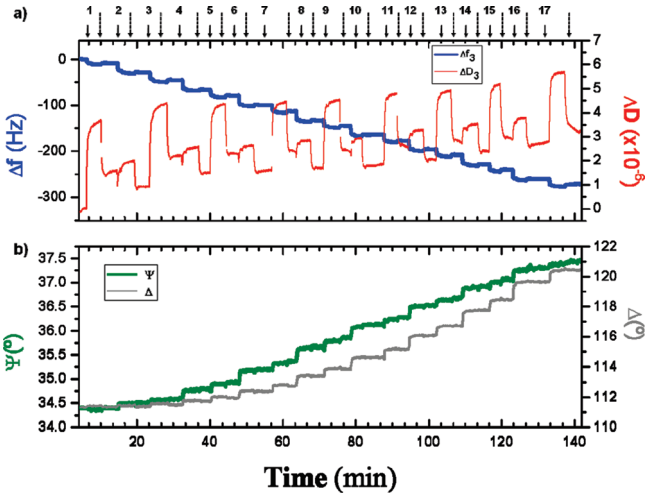

Figure 1. Assembly of 17 layers of PAH and PSS followed in situ by the combined QCM-D/ellipsometry device. (a) QCM-D response, i.e., Δf and ΔD vs time for a selected overtone ($i = 3$). (b) Ellipsometric response, i.e., ψ and Δ vs time for a selected wavelength ($\lambda = 632.5$ nm). The starting time of each deposition step and rinses are indicated by solid and dashed arrows, respectively, together with the step number. Odd and even numbers correspond to the incubation of PAH and PSS, respectively.

for d_{opt} and $n_{PEM} - n_{solvent}$ are quite sensitive to minor variations in the optical properties of the solid support. When discussing our results in terms of thickness, we will therefore consider d_{QCM} rather than d_{opt}. The errors in d_{opt} and n_{PEM}-$n_{solvent}$ are though covariant; i.e., the product $d_{opt} \times (n_{PEM} - n_{solvent})$ and m_{opt} can be determined with good accuracy.[14] The experimental noise was typically below 1 ng/cm^2.

Quantification of the Aqueous Solvent Content. The masses determined by QCM-D and ellipsometry, respectively, can be employed to calculate the solvent content of the film. To this end, we define the hydration as the percentage of solvent contributing to the total film mass:

$$\text{hydration (\%)} = \frac{m_{QCM} - m_{opt}}{m_{QCM}} \times 100 = \frac{m_{sol}}{m_{QCM}} \times 100. \quad (4)$$

Results

Assembly of PEMs Made of PAH and PSS. Figure 1 illustrates the in situ combined QCM-D/ellipsometry measurements for the assembly of 17 layers of PAH and PSS in 0.5 M NaCl. Figure 1a shows the variations in frequency and dissipation recorded by the QCM-D device. The dissipation shift remained low throughout the entire assembly process, indicating the formation of a rather rigid film. For such a film, the Sauerbrey equation is clearly applicable to calculate the increase in total film mass (including solvent), or m_{QCM}, after each deposition step. The polymer mass, or m_{opt}, was obtained from the fitting of the real-time variation of ψ and Δ measured along the multilayer deposition (Figure 1b).

The calculated values for the acoustic thickness (d_{QCM}) and both m_{opt} and m_{QCM} are shown in Figure 2 as a function of the number of assembled layers. PAH/PSS PEMs have previously been reported to exhibit linear growth,[41] and our results confirm this tendency.

The thickness of the PAH/PSS multilayer (Figure 2a) increased linearly, at a rate of 6.4 nm per PAH/PSS incubation cycle. Interesting features arise from the analysis of plots, regarding in situ variations of m_{opt} and m_{QCM} as shown in Figure 2b. Across the first three incubation steps, the polymer mass (m_{opt}) increased more slowly than the total film mass (m_{QCM}), while the increase rate was comparable for all subsequent incubation steps. It is noticeable that the increase in m_{opt} of the first layer is very small, 0.021 μg/cm^2 while the m_{QCM} for this layer is 0.213 μg/cm^2. This means that around the 90% of the total mass corresponds to water or aqueous solution (Figure 3). The sensed mass of water

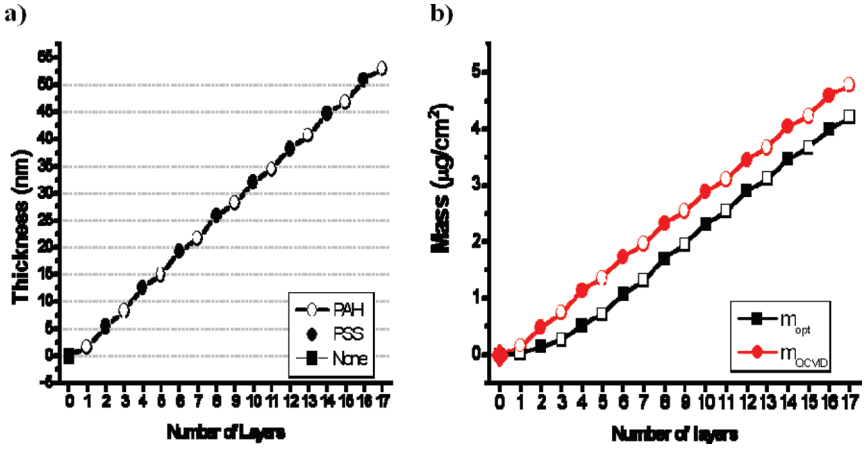

Figure 2. Evolution of the total film thickness (a) and the adsorbed masses (b) as a function of the number of deposited layers of PAH and PSS. Both m_{opt} (squares), which reflects the pure polymer mass, and m_{QCM} (circles), which includes solvent in the film, are displayed. Open and filled symbols indicate adsorption of the polycation or the polyanion, respectively.

may either represent water molecules bound to polymer chains or water that is entrapped between chains or layers. It has previously been reported that the first layers of PAH/PSS do not form a homogeneous film and assemble into islands that cover the surface heterogeneously.[42,44] A part of the solvent that is situated in the interstices between these islands will also contribute to m_{QCM}.[43] After the third layer, both m_{opt} and m_{QCM} increased by around 0.2 μg/cm^2 for every PAH layer added, and around 0.4 μg/cm^2 for every PSS layer. Concomitantly, the hydration of the multilayer (Figure 3) continuously decreased along with the number of layers assembled, reaching a value of only 12% after the final 17th layer. An overall densification of the multilayer with increasing number of layers can be inferred.[45]

It is quite remarkable that, for more than three layers, the *absolute* amount of water in the PEM did not depend on the number of deposited layer pairs. The global structure of sufficiently thick PEMs has previously been conceptualized by a three-zone model: two interfacial zones, which are affected by the presence of the solid support and the bulk solution, respectively, and maintain a constant thickness; and an interior zone, placed between the two interfacial ones, that grows in thickness as additional layers are deposited.[13] Our observation that the absolute amount of water in the PEM is constant indicates that the interior zone is essentially water free and that water is primarily entrapped in the interfacial zones. The change in the water content when passing from even to odd layers suggests that at least some of that water must be situated in the interfacial zone adjacent to the bulk solution. Then, the small differences in water content between PEMs with PAH as last layer and PEMs with PSS as last layer, are due to the particular hydration of the last layer. Clearly, the presence of NaCl retains PAH and PSS in a strongly collapsed state inside the PEM. We can associate the presence of water to the uncompensated charges present in the last layers of the PEM.

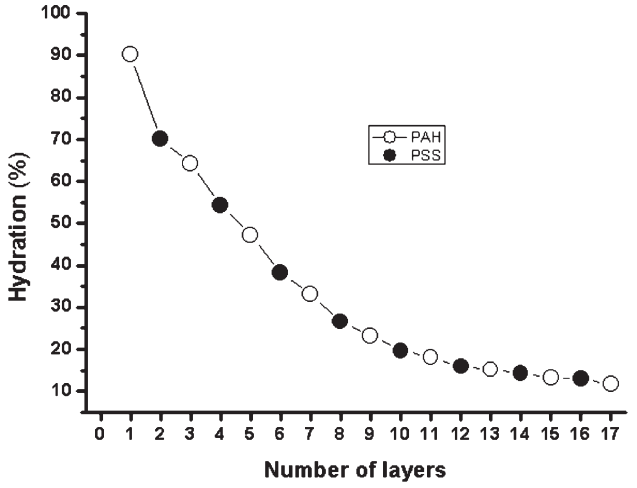

Figure 3. Aqueous solvent content as a function of the number of deposited layers of PAH (open circles) and PSS (filled circles).

For comparison, PAH/PSS multilayers were also assembled following a protocol that included the washing with water between the layer deposition steps. The variations in m_{opt} (Figure 4a) were identical to the values obtained with NaCl washings (Figure 2b). The values for m_{QCM}, in contrast, diverged significantly from those previously observed. Starting with the third layer, m_{QCM} increased more strongly than m_{opt}. The divergence between m_{QCM} and m_{opt} provides evidence that the modified deposition procedure leads to the entrapment of water in the PEM. Figure 4b illustrates that the hydration approaches a final value of 43%; i.e., almost half of the PEM mass is water. Assuming equimolar polyanion and polycation content, this corresponds to a ratio of seven water molecules per polyelectrolyte monomer. It is interesting that the PAH/PSS PEM soaks more water with increasing layer number when rinsing with water, although the amounts of PAH and PSS that bind per incubation step remain constant. Two scenarios appear plausible to explain this effect. One could assume that while charges are compensated in the interior of the multilayer, the last layer behaves as a polyion and hence soaks water upon reduction of the ionic strength. In this case, the hydration would be coming only from the last layer of the PEM, and the capacity of this last layer to soak water increases with layer number; i.e., the arrangement of the chains as the film grows becomes more favorable for the swelling of the last layer. Alternatively, it may be the interior of the PEM and not only the last layer that swells during the rinsing with pure water. The weak dependence of the water content on the number of exposure cycles for sufficiently large number of layers and the linear growth make the latter scenario more likely.

Assembly of PEMs Made of PDADMAC and PSS. The in situ combination of QCM-D with ellipsometry was then applied to study the growth of PEMs of a total of 17 layers

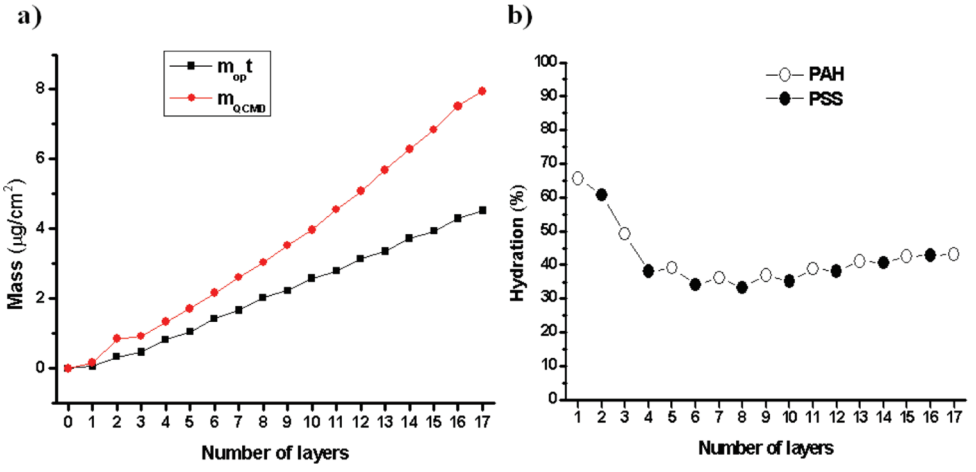

Figure 4. (a) m_{QCMD} (circles) and m_{opt} (squares) values for PAH/PSS assembly with washes in pure water between deposition steps. (b) Hydration plot of the PAH/PSS PEM as a function of the layer number. Open and filled symbols indicate the adsorption of the polycation and the polyanion, respectively.

composed of PDADMAC as polycation and PSS as polyanion, with washes in 0.5 M NaCl between the incubation steps. Figure 5 shows the responses in the acoustic parameters, Δf and ΔD, and optical parameters, ψ and Δ, measured for this system.

Compared to the frequency shifts, which reached values of -750 Hz, the dissipation shifts remained small, 4.5×10^{-6}, indicating the formation of an overall rather rigid film. It is notable that the incubation with polyelectrolyte solution induced a rather strong increase in ΔD that was partly reversed after rinsing in salt solution. Furthermore, the dissipation after incubation of the PEM with PDADMAC was always larger, and the film hence softer, than after exposure to PSS. We note also that the time needed to reach equilibrium in ΔD upon rinsing were rather long, while the optical responses and Δf equilibrated quickly. These observations suggest a rather strong reorganization of the PEM. Thickness, m_{opt} and m_{QCM} were calculated from the raw data for the assembly of the PDADMAC/PSS multilayer (Figure 6).

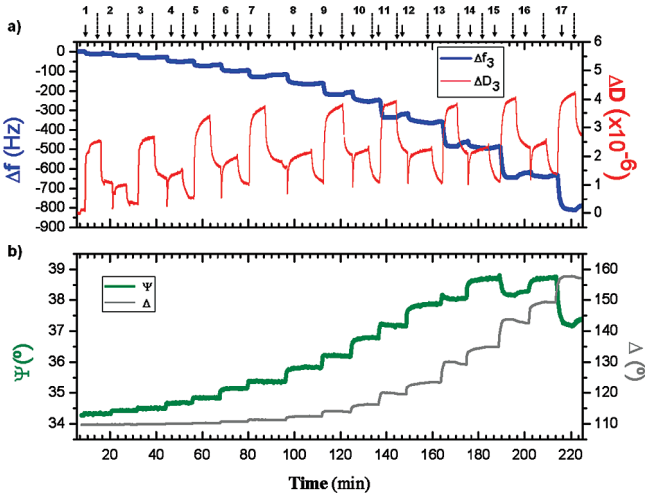

Figure 5. Assembly of 17 layers of PDADMAC and PSS in 0.5 M NaCl followed in situ by the combined QCM-D/ellipsometry device. (a) QCM-D response, i.e., Δf and ΔD vs time for a selected overtone ($i = 3$). (b) Ellipsometric response, i.e., ψ and Δ vs time for a selected wavelength ($\lambda = 632.5$ nm). The starting time of each deposition step and rinses are indicated by solid and dashed arrows, respectively, together with the step number. Odd and even numbers correspond to the incubation of PDADMAC and PSS, respectively.

After 17 layers, the film reached a thickness of 157 nm (Figure 6a). From the 11th layer onward the odd layer numbers, which correspond to PDADMAC, resulted always in more significant increases in the thickness values than the increases observed for even layers, corresponding to PSS. Both m_{QCM} and m_{opt} clearly exhibit supralinear growth (Figure 6b). A semilogarithmic plot of these quantities (Figure 6, inset), however, does not show a clear linear dependence of log(m) on layer number. The PEM growth is hence not strictly exponential. A total mass of 14.1 μg/cm^2 and a polymer mass of 8.5 μg/cm^2 (Figure 6b) were calculated from acoustic and optical data, respectively.

An interesting feature of the mass curves in Figure 6b is their diverging growth behavior, which becomes particularly apparent at large layer numbers. Upon deposition of PDADMAC, the increase in m_{QCM} is large and the increase is m_{opt} is rather small. The opposite situation is observed upon deposition of PSS. This translates into a hydration curve (Figure 7a) that oscillates, starting at the ninth assembly step, between values of a maximum of 40−45% and a minimum of 30−35%.

The hydration plot also reveals that, when considering odd and even layer numbers separately, the water content decreased throughout the buildup of the PEM. For thick PEMs, the hydration approached plateaus of about 30 and 40% for final incubations with PSS and PDADMAC, respectively. This implies that the amount of assembled polyelectrolyte increased proportionally to the amount of water entrapped. Assuming that the film contains an equimolar amount of cationic and anionic groups, the ratio of water molecules per polyelectrolyte monomer for thick PEMs can be calculated to oscillate between 5:1 and 7:1 for PEMs with PSS and PDADMAC as last layers, respectively. These values might have an over- or underestimation, of at most ±13%, if PDADMAC or PSS, respectively, were the last assembled layer.

We also calculated the increment in both net polymer and total film mass for each incubation step (Figure 7b,c). Clearly, the increments in total mass upon assembly of PDADMAC increase strongly with layer number, while the increments in net polymer mass seem to have attained a plateau. For PSS, in contrast, the increments in net

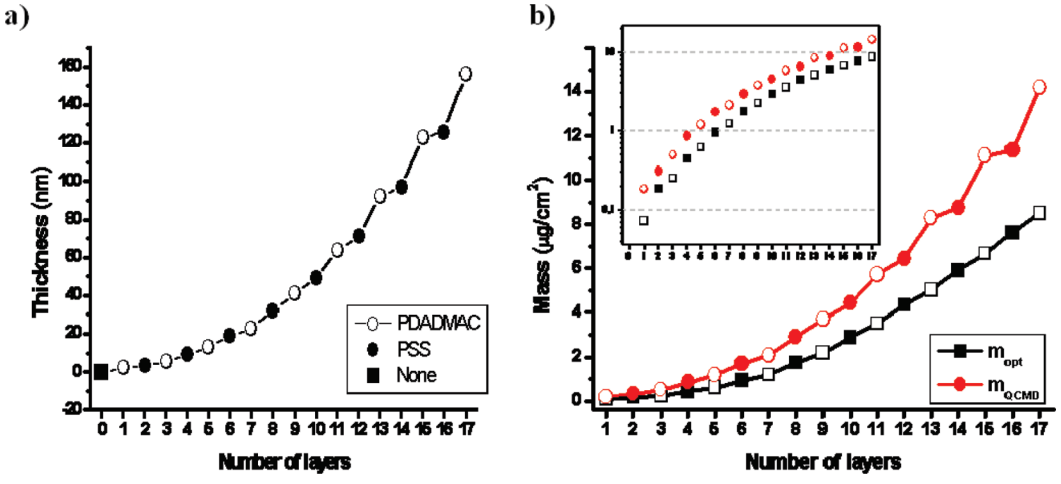

Figure 6. PEM composed of PDADMAC and PSS with a total of 17 layers built in 0.5 M NaCl. (a) Thickness variation per layer assembled. (b) Comparison between m_{opt} (squares) and m_{QCM} (circles) as a function of layer number. The inset shows the same date in a semilogarithmic plot. Open and filled symbols indicate adsorption of the polycation or the polyanion, respectively.

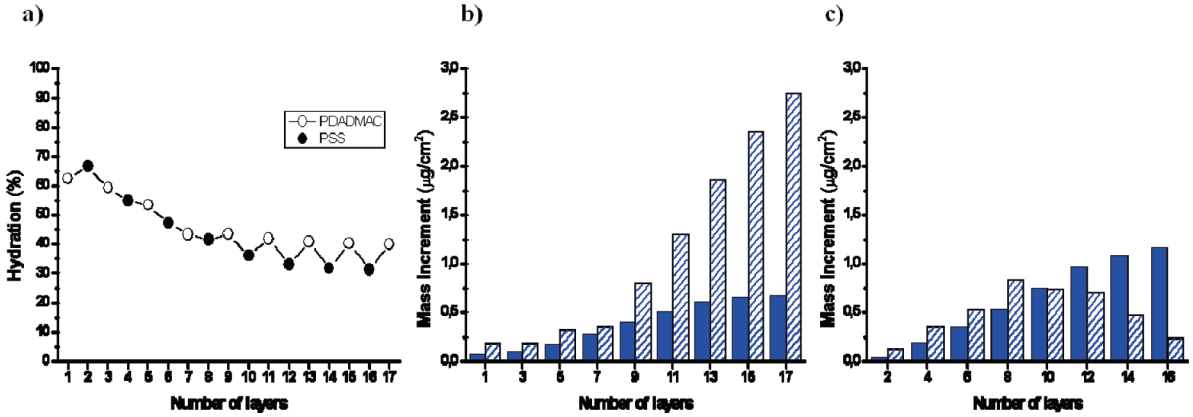

Figure 7. (a) Aqueous solvent content in the film vs number of deposited layers of PDADMAC (open circles) and PSS (filled circles) plot. Increments in m_{opt} (solid bars) and m_{QCM} (hatched bars) upon deposition of PDADMAC (b) and PSS (c) for a PDADMAC/PSS multilayer grown with 0.5 M NaCl washing steps.

polymer mass increase monotonously, while the increments in total mass decrease after reaching a maximum at layer number 8.

As a comparison with the PAH/PSS PEM, we also assembled PDADMAC and PSS by using pure water instead of NaCl solution for the washing between each layer deposition (Figure 8). From the inspection of the dissipation shifts, drastic changes in the mechanical properties of the multilayer as a function of the salt concentration in solution can be deduced. In NaCl solutions, the dissipation shifts remained small, at levels that are comparable to those in Figure 5. Exchange of the bulk solution to pure water, however, induced drastic increases in ΔD, indicating a softening of the film. The changes in dissipation were particularly significant for PEMs with PDADMAC as the last layer. Here, the changes in dissipation when changing the solvent increased strongly as the buildup of the multilayer proceeded, reaching values of 100×10^{-6} and more. The strong dissipation shifts were accompanied by strong frequency shifts, indicating that hydration/swelling is responsible for the softening of the film.

Figure 9 shows the variations of d_{QCM}, m_{opt}, and m_{QCM} along the multilayer buildup. With the protocol including water rinsing, the PDADMAC/PSS multilayers showed an initial exponential growth of m_{QCM} until the ninth layer, which was followed by strong oscillations in the mass. After 17 incubation steps, a film thickness of 370 nm was reached, which is twice the value observed in NaCl solution. The total film mass also doubled. In contrast, the polymer mass was only marginally affected by the change in the rinsing method throughout the entire PEM buildup. The oscillatory behavior that we found for m_{QCM} is also apparent for the thickness of the multilayer (Figure 9a), illustrating the cycles of swelling and shrinkage that ensue upon deposition of PDADMAC and PSS, respectively. An oscillatory behavior is also evident for the polymer mass, albeit to a lesser degree. Notably, the oscillation of m_{QCM} is out of phase with the oscillation of m_{opt}, i.e., a maximum in m_{QCM} coincides with a minimum in m_{opt}.

The comparison of Figure 10a with Figure 7a demonstrates that the hydration was dramatically affected by the change in the protocol of assembly. Except for the first layer, the hydration after rinsing with water remained approximately constant, at about 50%, up to the seventh layer. Then, the hydration started to oscillate, between about 30% and 70%, upon assembly of PSS and PDADMAC, respectively. Assuming again equimolar presence of cations and anions in the film, the ratio of water molecules per polyelectrolyte monomer reached 29:1 for the swollen PEMs after assembly of PDADMAC and diminished to 4:1 for the compact films after PSS assembly.

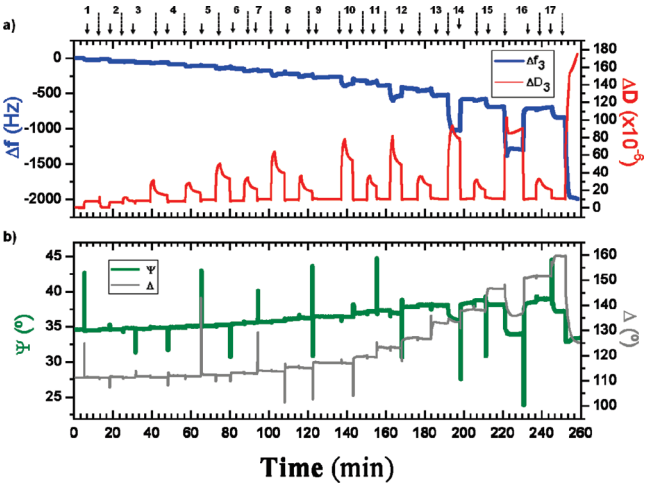

Figure 8. Assembly of 17 PDADMAC/PSS layers with washes in pure water followed in situ by the combined QCM-D/ellipsometry device. (a) QCM-D response, i.e., Δf (blue line) and ΔD (red line) vs time for a selected overtone ($i = 3$). (b) Ellipsometric response, i.e., ψ (green line) and Δ (gray line) vs time for a selected wavelength ($\lambda = 632.5$ nm). The starting time of each deposition step and rinses are indicated by solid and dashed arrows, respectively, together with the step number. Odd and even numbers correspond to the assembly of PDADMAC and PSS, respectively. The strong but transient peaks in the ellipsometric response are artifacts that originate from strong scattering of light upon exchange of pure water against polymer-containing NaCl solutions.

As for the PEM with washing steps of 0.5 M NaCl between layers, we have also determined the mass increments corresponding to each assembled layer for both m_{opt} and m_{QCM} (Figure 10b,c). For PDADMAC, constant increments in m_{opt} of 0.2−0.3 $\mu g/cm^2$ were observed until the ninth layer. For the following layers, very small or even negative increments were found. This net loss of polymer mass most likely indicates removal of PSS from the PEM upon exposure of PDADMAC. At the same time, the increments in m_{QCM} became progressively bigger, with typically more than 2-fold increases from one assembly step to the next. The mass increments for PSS followed a very different trend. The increments in m_{QCM} were initially constant, at 0.5−0.7 $\mu g/cm^2$, became zero at layer 10, and then decreased strongly. In contrast, m_{opt} increased progressively.

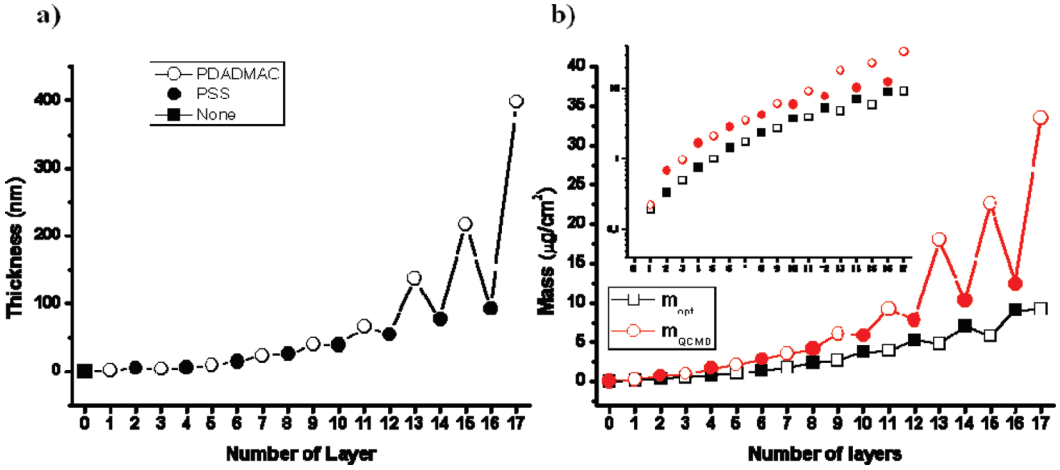

Figure 9. PEM composed of PDADMAC and PSS with a total of 17 layers built with washes in pure water. (a) Evolution of the total film thickness. (b) Comparison between m_{opt} (black squares) and m_{QCM} (red circles) as a function of layer number. The inset shows the same date in a semilogarithmic plot. Open and filled symbols indicate adsorption of the polycation or the polyanion, respectively.

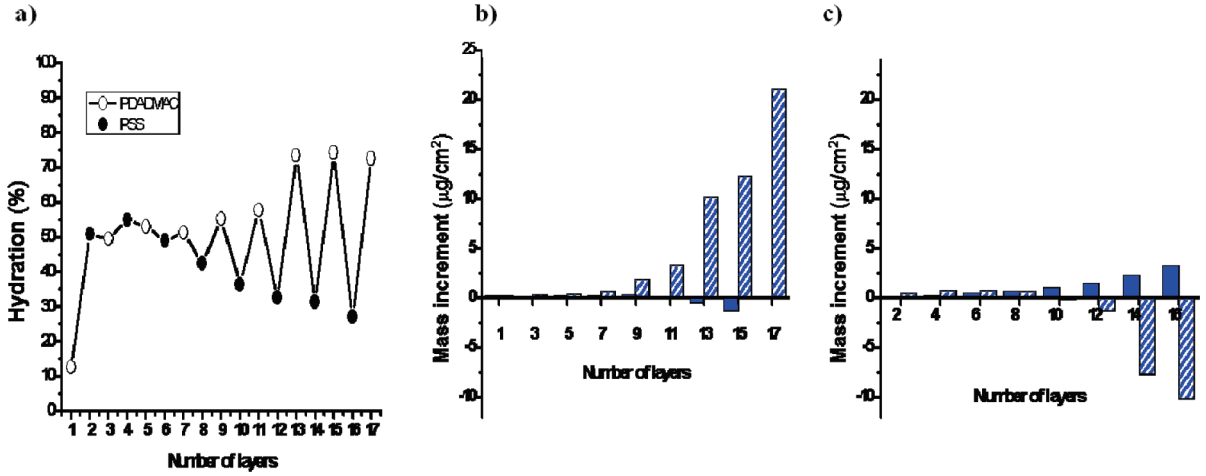

Figure 10. (a) Aqueous solvent content in the film vs number of deposited layers of PDADMAC (open circles) and PSS (filled circles). Increments in m_{opt} (solid bars) and m_{QCM} (hatched bars) upon deposition of PDADMAC (b) and PSS (c) for a PDADMAC/PSS multilayer grown with pure water washing steps.

Undoubtedly, the hydration of the PDADMAC/PSS PEMs is strongly affected by the ionic strength of the washing solution. It is known that the ionic strength has a direct impact on the conformation of the assembled layers. We find that the PDADMAC/PSS multilayer behaves as a swollen polymer matrix that looses water as the ionic strength increases. The extent of water loss from the film makes us think that it is acting like a salt-sensitive hydrogel that responds osmotically to the ionic strength, soaking water up to 70% of the total multilayer mass in conditions of low ionic strength.

To observe this effect directly, we exposed the PDADMAC/PSS multilayer built in NaCl to a water rinse (data not shown). While the 17 layer PEM had a thickness of around 160 nm and a water content of 37% in 0.5 M NaCl, a thorough water rinse made the multilayer change to a thickness of 360 nm and to a water content of 77%. These values are very similar to those observed for the multilayer built with water washes (Figures 9 and 10). Both Δf and ΔD recovered their original value after returning to 0.5 M NaCl, providing evidence that the salt-dependent swelling is a reversible process. However, repeating the same exposure to water for the PAH/PSS multilayer built in NaCl did not show any dramatic effect on the system.[46]

The addition of PSS had a dramatic effect on the water content in the PDADMAC/PSS PEMs. The hydration decreased to values that were comparable to those observed for PEMs build with rinses with salt solution, indicating that the sensitivity to salt is drastically reduced. The cycling between a salt-responsive hydrogel after exposure to PDADMAC and a salt-insensitive film after exposure to PSS must be the result of a particular arrangement of polyelectrolytes in the PEM. The responsiveness to salt after addition of PDADMAC indicates (i) that a large amount of charges has become available in the PEM and (ii) that the internal structure of the PEM readily allows for molecular rearrangements. At least one of these two properties appears to be temporarily lost upon addition of PSS; i.e., PSS must act either by neutralizing charges or by locking the special arrangement of polyelectrolyte monomers, or both.

One might wonder if the reversible change from a salt-responsive to a salt-insensitive structure occurs within the entire PEM, or at least a substantial part of it, or if it occurs exclusively within the interfacial zone between the PEM and the bulk solution. Diffusion of one or both polyelectrolytes into the interior of the PEM has previously been observed and related to exponential growth.[15] In our films, we observe supralinear, albeit not strictly exponential, growth. An

alternative scenario would be that the interfacial zone increases in thickness with the increasing number of assembly steps. At present, we cannot exclude either of these two possibilities. Besides the diffusion proposed to explain the exponential growth, it has to be taken into account that there is an interdigitation of the polyelectrolyte layers and it has been proposed that an assembled layer extents up to 4−5 layers below. Therefore, even if the phenomena that have been described take place at the interfacial zone they could be involving several layers below.[47]

Conclusions

We have been able to follow simultaneously, by spectroscopic ellipsometry and QCM-D in a single combined device, the growth of PDADMAC/PSS and PAH/PSS multilayers. The combination of ellipsometry and QCM-D allows studying how the hydration of the PEMs varies throughout the assembly process. Our data illustrate that the buildup and the evolution of the water content in PEMs are tightly connected. The combination of both techniques in a single device is hence extremely useful to study the mechanism of assembly of such systems.

We observe drastic differences in the hydration behavior of PAH/PSS and PDADMAC/PSS PEMs, which must originate from the differences in the interaction between the two polycations and PSS, and in the structure of the films formed. The linearly growing PAH/PSS PEMs produced a film that contained almost no water in its interior when assembled with rinses in salt solution, while assembly with rinses in pure water produced a film that contained more than 40% water. PDADMAC/PSS PEMs showed supralinear growth. They exhibited strong (up to 2-fold) and fully reversible swelling as a function of the salt concentration with water contents reaching values of 70% and more, if the last incubation step was with PDADMAC.

Acknowledgment. R.P.R. acknowledges funding from the German Federal Ministry of Education and Research (BMBF, project 0315157), the Spanish Ministry of Science and Innovation (MICINN, refs MAT2008-04192 and RYC2009-04275), and the Department of Industry of the Basque Government. S.M. acknowledges support from the Spanish Ministry of Science and Innovation (MAT2007-0458) and the Ramon y Cajal program as well as support from the Department of Industry of the Basque Government.

References and Notes

(1) Decher, G.; Hong, J. D.; Schmitt, J. *Thin Solid Films* **1992**, *210−211*, 831–835.
(2) Decher, G. *Science* **1997**, *277*, 1232–1237.
(3) Arys, X.; Laschewsky, A.; Jonas, A. M. *Macromolecules* **2001**, *34*, 3318–3330.
(4) Sukhorukov, G. B.; Donath, E.; Lichtenfeld, H.; Knippel, E.; Knippel, M.; Budde, A.; Möhwald, H. *Colloids Surf., A* **1998**, *137*, 253–266.
(5) Donath, E.; Sukhorukov, G. B.; Caruso, F.; Davis, S. A.; Möhwald, H. *Angew. Chem., Int. Ed.* **1998**, *37*, 2201–2205.
(6) Yaroslavov, A. A.; Rakhnyanskaya, A. A.; Yaroslavova, E. G.; Efimova, A. A.; Menger, F. M. *Adv. Colloids Interface Sci.* **2008**, *142*, 43–52.
(7) Grigoriev, D. O.; Köhler, K.; Skorb, E.; Shchukin, D. G.; Möhwald, H. *Soft Matter* **2009**, *5*, 1426–1432.
(8) Jin, W.; Toutianoush, A.; Tieke, B. *Langmuir* **2003**, *19*, 2550–2553.
(9) Rmaile, H. H.; Schlenoff, J. B. *J. Am. Chem. Soc.* **2003**, *125*, 6602–6603.
(10) Llarena, I.; Iturri Ramos, J. J.; Donath, E.; Moya, S. E. *Macromol. Rapid Commun.* **2010**, *31*, 526–531.
(11) Dubas, S. T.; Kittitheeranun, P.; Rangkupan, R.; Sanchavanakin, M.; Potiyaraj, P. *J. Appl. Polym. Sci.* **2009**, *114*, 1574–1579.
(12) Cai, G.; Lee, W.; Min, S. K.; Koo, G.; Cho, B. W.; Lee, S. H.; Han, S. H. *J. Nanosci. Nanotechnol.* **2009**, *9*, 7209–7214.
(13) Ladam, G.; Schaaf, P.; Voegel, J. C.; Schaaf, P.; Decher, G.; Cuisinier, F. *Langmuir* **2000**, *16*, 1249–1255.
(14) Caruso, F.; Niikura, K.; Furlong, D. N.; Okahata, Y. *Langmuir* **1997**, *13*, 3422–3426.
(15) Lavalle, P.; Gergely, C.; Cuisinier, F. J. G.; Decher, G.; Schaaf, P.; Voegel, J. C.; Picart, C. *Macromolecules* **2002**, *35*, 4458–4465.
(16) Hübsch, E.; Ball, V.; Senger, B.; Decher, G.; Voegel, J. C.; Schaaf, P. *Langmuir* **2004**, *20*, 1980–1985.
(17) Picart, C.; Mutterer, J.; Richert, L.; Luo, Y.; Prestwich, G. D.; Schaaf, P.; Voegel, J. C.; Lavalle, P. *Proc. Natl. Acad. Sci. U.S.A.* **2002**, *99*, 12531–12535.
(18) Guzman, E.; Ritacco, H.; Rubio, J. E. F.; Rubio, R. G.; Ortega, F. *Soft Matter* **2009**, *5*, 2130–2142.
(19) Liu, G.; Zou, S.; Fu, L.; Zhang, G. *J. Phys. Chem. B* **2008**, *112*, 4167–4171.
(20) Salomäki, M.; Vinokurov, I. A.; Kankare, J. *Langmuir* **2005**, *21*, 11232–11240.
(21) Marx, K. A. *Biomacromolecules* **2003**, *4*, 1099–1120.
(22) Notley, S. M.; Eriksson, M.; Wagberg, L. *J. Colloid Interface Sci.* **2005**, *292*, 29–37.
(23) Iturri Ramos, J. J.; Llarena, I.; Fernandez, L.; Moya, S. E.; Donath, E. *Macromol. Rapid Commun.* **2009**, *30*, 1756–1761.
(24) Schonhoff, M.; Ball, V.; Bausch, A. R.; Dejugnat, C.; Delorme, N.; Glinel, K.; von Klitzing, R.; Steitz, R. *Colloids Surf., A* **2007**, *303*, 14–29.
(25) Schlenoff, J. B.; Rmaile, A. H.; Bucur, C. B. *J. Am. Chem. Soc.* **2008**, *130*, 13589–13597.
(26) Haberska, K.; Ruzgas, T. *Bioelectrochemistry* **2009**, *76*, 153–161.
(27) Gong, X.; Gao, C. *Phys. Chem. Chem. Phys.* **2009**, *11*, 11577–11586.
(28) McCrackin, F. L.; Passaglia, E.; Stromberg, R. R.; Steinberg, H. L. *J. Res. Natl. Bur. Stand.,A.* **1963**, *67A*, 363–377.
(29) Cuypers, P. A.; Corsel, J. W.; Janssen, M. P.; Kop, J. M. M.; Hermens, W. T.; Hemker, H. C. *J. Biol. Chem.* **1983**, *258*, 2426–2431.
(30) Halthur, T. J.; Elofsson, U. M. *Langmuir* **2004**, *20*, 1739–1745.
(31) Mauser, T.; Déjugnat, C.; Sukhorukov, G. B. *Macromol. Rapid Commun.* **2004**, *25*, 1781–1785.
(32) Köhler, K.; Shchukin, D. G.; Möhwald, H.; Sukhorukov, G. B. *J. Phys. Chem. B* **2005**, *209*, 18250–18259.
(33) Sauerbrey, G. *Z. Phys.* **1959**, *155*, 206–222.
(34) Domack, A.; Prucker, O.; Rühe, J.; Johannsmann, D. *Phys. Rev.* **1997**, *56*, 680–689.
(35) Voinova, M. V.; Rodahl, M.; Jonson, M.; Kasemo, B. *Phys. Scr.* **1999**, *59*, 391–396.
(36) Eisele, N. B.; Frey, S.; Piehler, J.; Görlich, D.; Richter, R. P. *EMBO Rep.* **2010**, *11*, 366–372.
(37) Carton, I.; Brisson, A. R.; Richter, R. P. Submitted for publication
(38) Daimon, M.; Masumura, A. *Appl. Opt.* **2007**, *46*, 3811–3820.
(39) Lide, D. R. *Handbook of Chemistry and Physics*, 85th ed.; CRC Press: Boca Raton, FL, U.S.A., 2004.
(40) De Feijter, J. A.; Benjamins, J.; Veer, F. A. *Biopolymers* **1978**, *17*, 1759–1772.
(41) Dejeu, J.; Buisson, L.; Guth, M. C.; Roidor, C.; Membrey, F.; Charraut, D.; Foissy, A. *Colloids Surf., A* **2006**, *288*, 26–35.
(42) McAloney, R. A.; Sinyor, M.; Dudnik, U.; Goh, M. C. *Langmuir* **2001**, *17*, 6655–6663.
(43) Bingen, P.; Wang, G.; Steinmetz, N. F.; Rodahl, M.; Richter, R. P. *Anal. Chem.* **2008**, *80*, 8880–8890.
(44) Porcel, C.; Lavalle, P.; Ball, V.; Decher, G.; Senger, B.; Voegel, J. C.; Schaaf, P. *Langmuir* **2006**, *22*, 4376–4383.
(45) Estrela-Lopis, I.; Leporatti, S.; Clemens, D.; Donath, E. *Soft Matter* **2009**, *5*, 214–219.
(46) Iturri Ramos, J. J.; Llarena, I.; Moya, S. E. Manuscript in preparation.
(47) Caruso, F.; Lichtenfeld, H.; Donath, E.; Möhwald, H. *Macromolecules* **1999**, *32*, 2317–2328.